Inference of Latent Neural Field Intensities from Spatiotemporal Point-Process Observations

Michael Rule, David Schnoerr, Matthias Hennig, Guido Sanguinetti

School of Informatics, University of Edinburgh, Edinburgh, UK, EH8 9AB

1. 3-State model for waves in excitable medium

Three-state neural field model, Buice & Cowan '09 (1): complex wave patterns without inhibitory cells.

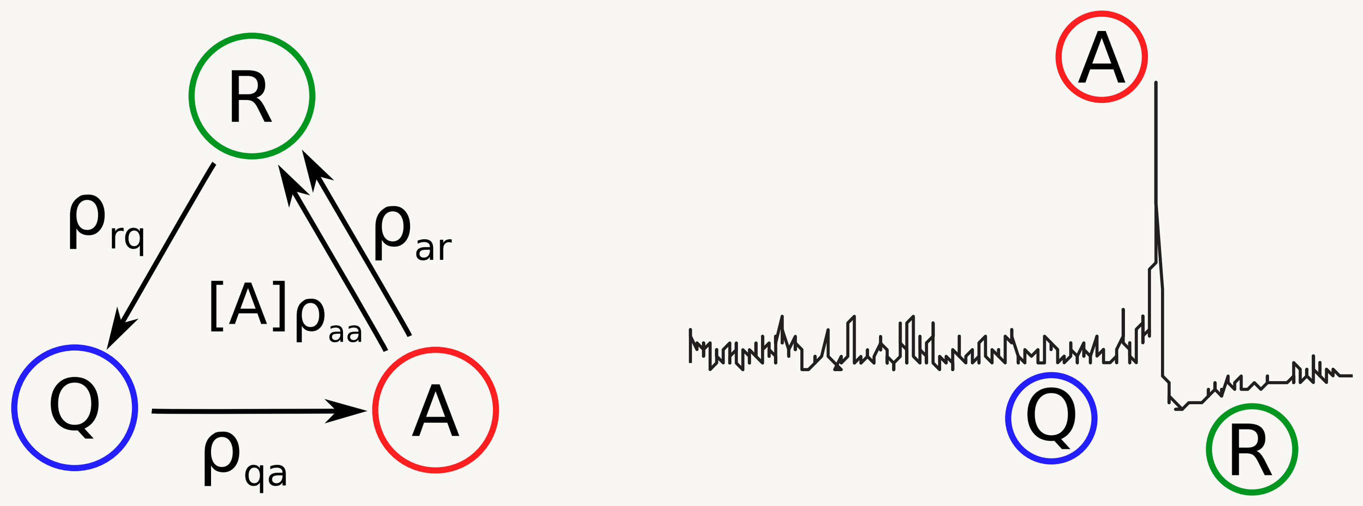

Figure 1. Quiescent-Active-Refractory (QAR) model of neural waves. The Q-A-R states (1) correspond to the Critical-Active-Stable retinal wave model of Hennig et al. '09 (2) and the Susceptible-Infected-Recovered model in epidemiology.

3 states

- **Q** Quiescent
- **A** Active
- **R** Refractory

4 rate parameters

- ρ_q Spontaneous spiking; Q to A ■ → ■
- ρ_a A to R transition ■ → ■
- ρ_r R to Q transition ■ → ■
- ρ_e Active cells excite Quiescent ■■ → ■■

Mean-field dynamics (exclude spontaneous $Q \to A$)

$$\dot{Q} = -\rho_e AQ + \rho_r R$$
$$\dot{A} = -\rho_a A + \rho_e AQ$$
$$\dot{R} = -\rho_r R + \rho_a A$$

Spontaneous $Q \to A$ sampled as shot noise (Poisson).

2. Spatial system

Let fields depend on coordinates (x, y) and define a lateral excitation kernel k with radius σ_i (*Nonlocal* interactions)

$$k(x, y) \propto \exp\left(-\frac{1}{2}\frac{x^2+y^2}{\sigma_i^2}\right)$$

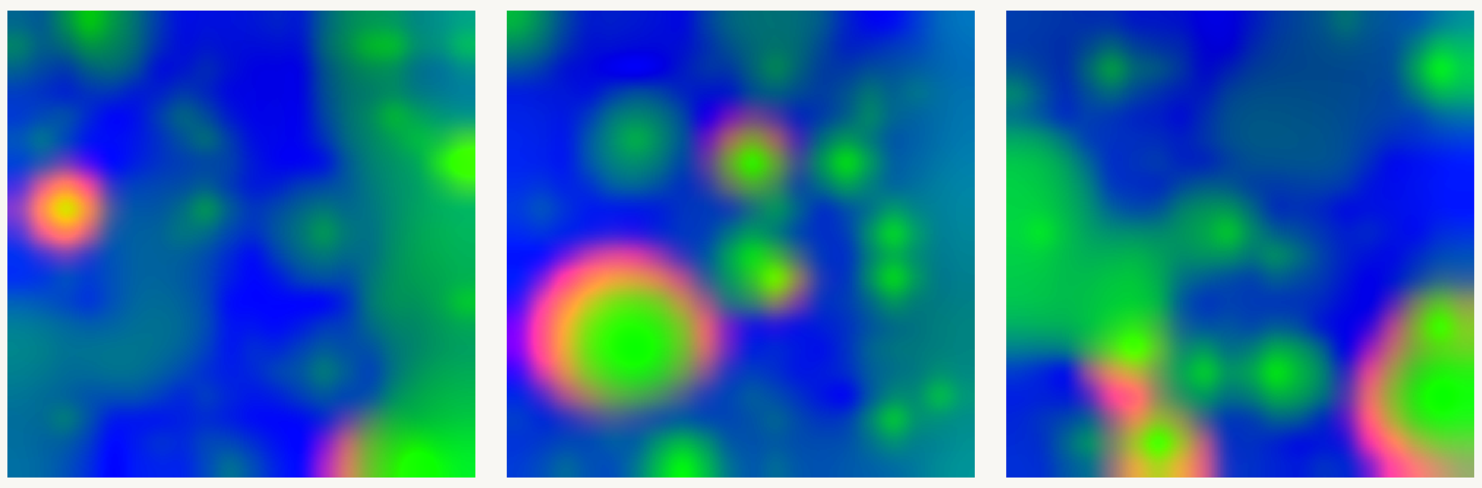

Figure 2. 3-state model can exhibit self-organized wave phenomena. Simulated on a $[0, 1]^2$ unit interval using 20x20 grid, σ=0.04, ρ_a=0.1, ρ_r=10^{-3}, ρ_e=0.4. Spontaneous excitation rate ρ_q=0.05. A finite threshold of 10^{-3} avoids widespread spontaneous excitation. Colors: Quiescent Active Refractory

3. Recover latent fields from spikes: Bayesian filtering

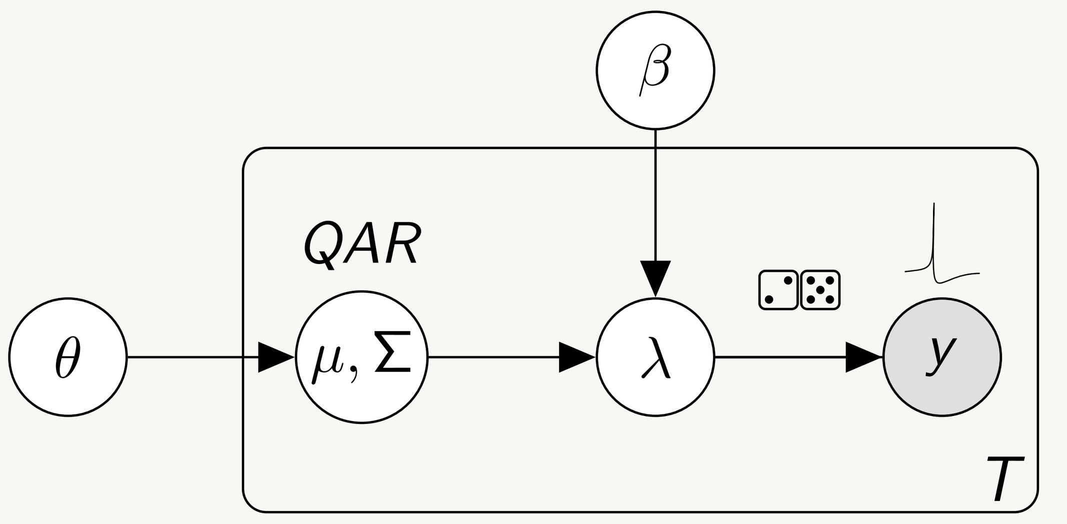

Figure 3. Hidden Markov model for latent neural fields. For all time-points T, state transition parameters θ=$(\rho_q, \rho_a, \rho_r, \rho_e, \sigma)$ dictate the evolution of a multivariate Gaussian model μ, Σ of latent fields Q, A, R. Observation model β is a linear map with adjustable gain and threshold, and reflects how field A couples to firing intensity λ. Point-process observations (spikes) y are Poisson with intensity λ.

Predict state:

- Multivariate Gaussian state-space model μ=(Q, A, R), covariance Σ
- Integrate forward μ mean-field equations
- Covariance Σ evolves according to the system Jacobian J
- Similar to continuous-time extended Kalman filter $\dot{\Sigma} = J\Sigma + \Sigma J^T + \Sigma_{\text{noise}}$

Measurement:

- Refine estimate using spiking observations
- Spikes: Poisson events with intensity $\lambda = mA + b$
- Posterior is proportional to product of predicted state and data likelihood
- Laplace approximation (gradient descent; constrain to positive field intensities)

4. Test case: developmental retinal waves

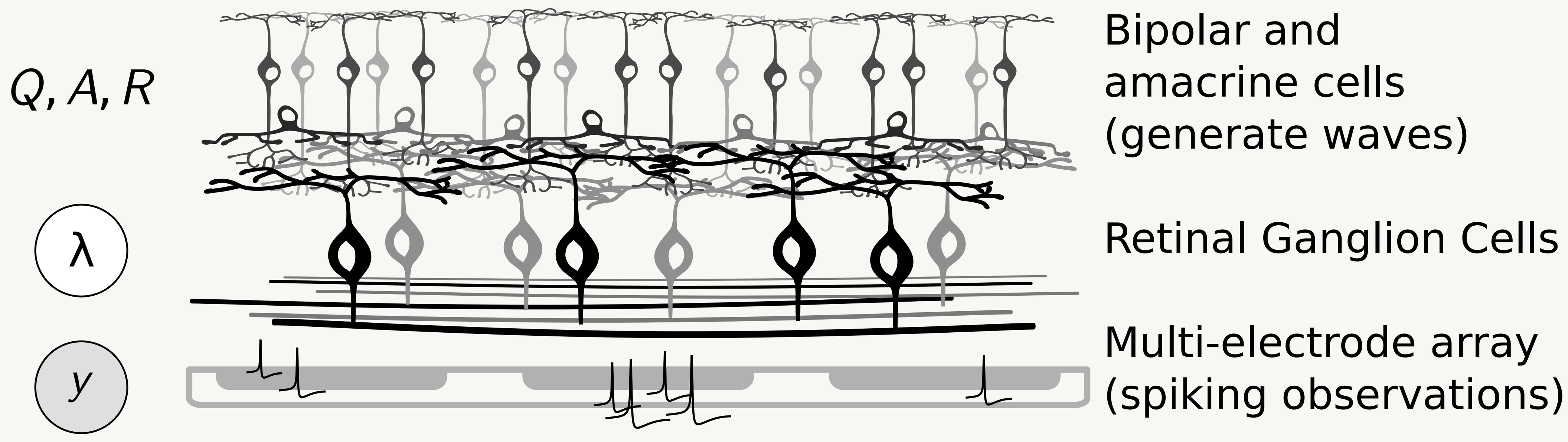

Figure 4. Illustration of inner retina and recording setup. Spontaneous retinal waves are generated in a layer of laterally interconnected amacrine cells. These waves activate Retinal Ganglion Cells (RGCs), the output cells of the retina. RGC electrical activity is recorded via a 64×64 multi-electrode array with 50 µm spacing.

High-density multielectrode array recordings of retinal waves

- 4096-electrode arrays, 42 µm spacing (3)
- Recordings courtesy of the Sernagor lab (4, 5)
- Spontaneous waves during development (6)
- Small events divide retina into refractory patches
- Rare large events sweep across the retina
- Self-organized structure at multiple scales (2)

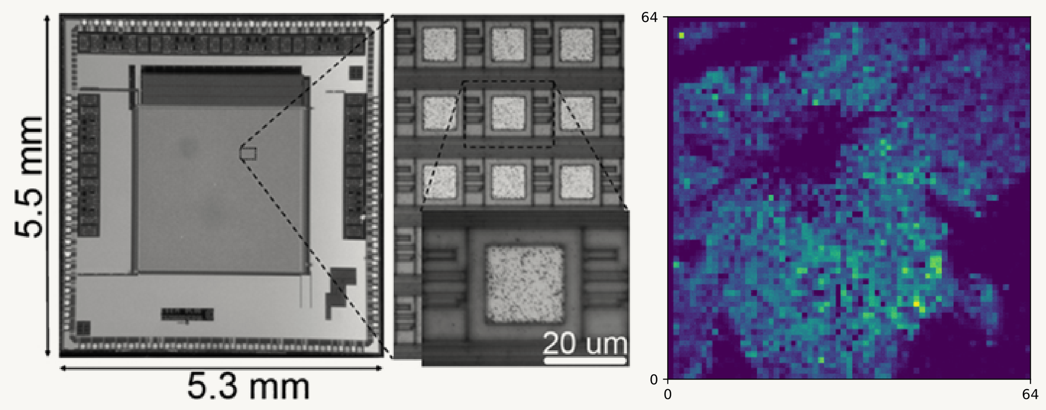

Figure 5. 4096-electrode array. *Left:* Array (3). *Right:* Spikes recorded in a single session.

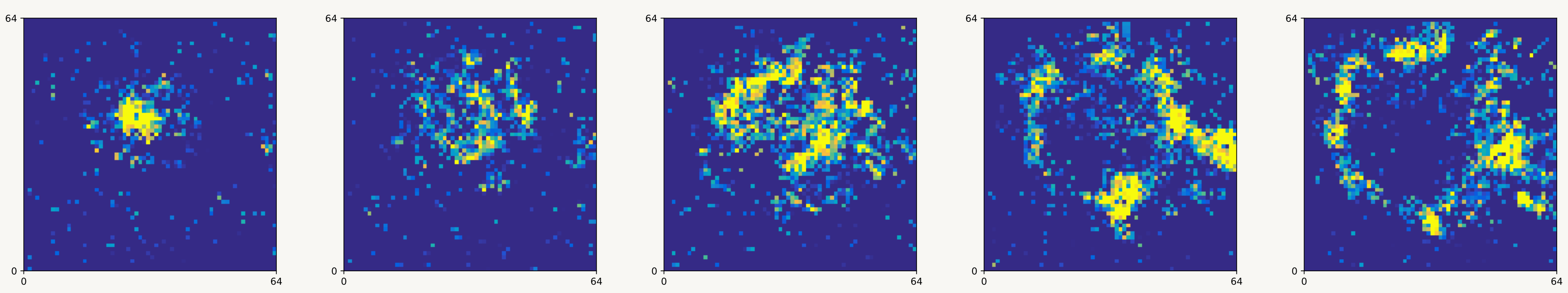

Figure 6. Example wave event, spike histograms in 1 s intervals. 2.6×2.6 cm^2. Mouse retina, postnatal day 11.

5. In practice

Numerically challenging:

- 3 states, 10×10 grid → 300-D covariance matrix (4.5k entries)
- *Avoid inverses*: work with inverse covariance (precision) matrix
- *Improve stability*: Cholesky factorization, triangular system solvers
- *Regularize* state variance

Performance e.g.:

- 37 s to filter 25 minutes of retinal data, Δt=1 *s*, ∼40 samples/s
- 10×10 grid; Matlab implementation, 2.9 GHz 8-core Xeon CPU
- Complexity dominated by matrix multiplication

Fluctuations:

- A model of fluctuations is needed to model uncertainty in state estimation
- Use a linear noise approximation of the original discrete system

$$\Sigma_{\text{noise}} = \begin{bmatrix} \rho_e AQ + \rho_r R & -\rho_e AQ & -\rho_r R \\ -\rho_e AQ & \rho_i A + \rho_e AQ & -\rho_i A \\ -\rho_r R & -\rho_i A & \rho_r R + \rho_i A \end{bmatrix}$$

6. Bayesian filtering recovers latent states

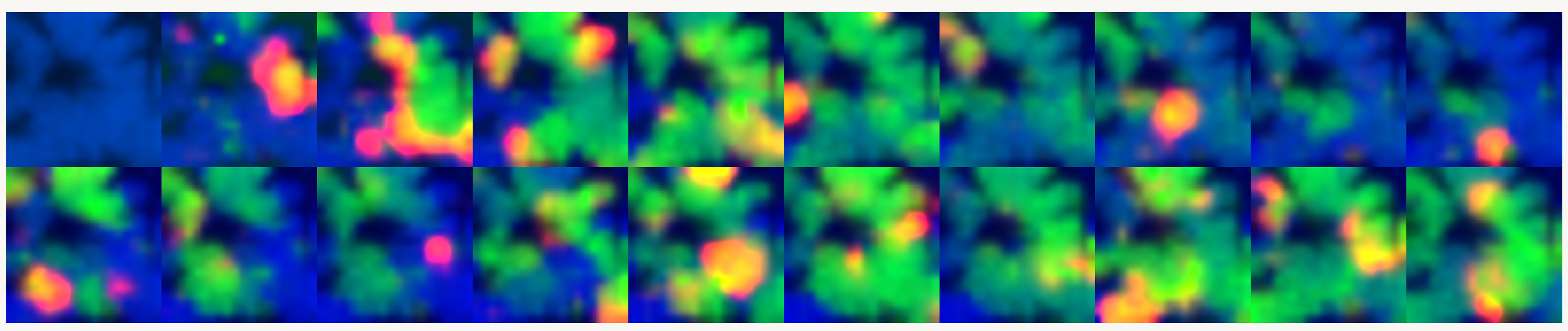

Figure 7. Filtering recovers wave states. Brightness ∝ cell density. Colors: Quiescent Active Refractory. Frames shown every 48 seconds; 2.6×2.6 cm^2 area; postnatal day 10; Multiscale "forest-fire like" waves.

Main points

- Spatiotemporal neural phenomena are complex: excitability, nonlinearity, refractoriness
- Previous spatiotemporal point-process inference procedures unsuitable (simple, linear)
- Three-state neural field model is suitable for inference
- Bayesian filtering recovers latent states, correlation structure, and model likelihood
- *Future:* model validation, forecasting, and control.

THE UNIVERSITY of EDINBURGH informatics

EPSRC Engineering and Physical Sciences Research Council

Sincere thanks to Evelyn Sernagor & Gerrit Hilgen for providing the retinal wave datasets.

Funding provided by EPSRC EP/L027208/1 *Large scale spatio-temporal point processes: novel machine learning methodologies and application to neural multi-electrode arrays*

[1] Buice MA et al. Statistical mechanics of the neocortex. *Progress in Biophysics and Molecular Biology*, 99(2-3):53–86, feb 2009. ISSN 00796107. doi: 10.1016/j.pbiomolbio.2009.07.003.

[2] Hennig MH, et al. Early-Stage Waves in the Retinal Network Emerge Close to a Critical State Transition between Local and Global Functional Connectivity. *Journal of Neuroscience*, 29(4), 2009.

[3] Imfeld K, et al. Large-scale, high-resolution data acquisition system for extracellular recording of electrophysiological activity. *IEEE Transactions on biomedical engineering*, 55(8):2064–2073, 2008.

[4] Muthmann JO, et al. Spike detection for large neural populations using high density multielectrode arrays. *Frontiers in neuroinformatics*, 9:28, 2015.

[5] Hilgen G, et al. Unsupervised spike sorting for large-scale, high-density multielectrode arrays. *Cell Reports*, 18(10):2521–2532, 2017.

[6] Maccione A, et al. Following the ontogeny of retinal waves: pan-retinal recordings of population dynamics in the neonatal mouse. *The Journal of Physiology*, 592(7):1545–1563, apr 2014. ISSN 00223751. doi: 10.1113/jphysiol.2013.262840.